

# Exploring the Impact of Chemical Composition on the Oxidation Resistance of 2000 Series Aluminum Alloys using Extreme Vertices Design

André da Silva Antunes<sup>a\*</sup> , Samuel Augusto Wainer<sup>b</sup>, João Guilherme Jacon de Salvo<sup>a,c</sup> 

<sup>a</sup>Instituto Tecnológico de Aeronáutica, Departamento de Materiais e Processos, São José dos Campos, SP, Brasil.

<sup>b</sup>Instituto Tecnológico de Aeronáutica, Departamento de Matemática, São José dos Campos, SP, Brasil.

<sup>c</sup>Instituto de Aeronáutica e Espaço, Divisão de Materiais, São José dos Campos, SP, Brasil.

Received: July 24, 2023; Revised: October 31, 2023; Accepted: November 30, 2023

This research investigates optimizing the properties of 2024 aluminum alloy using the Extreme Vertices Design (EVD) method and linear regression. It examines the oxidation behavior of the alloy during solubilization heat treatment, specifically focusing on the effect of magnesium addition leading to a dark oxide layer. The study employs a comprehensive experimental design and regression models to estimate the specific oxidation rate constant (k). Analysis of results reveals variations in oxidation behavior among alloys and the influence of aluminum, copper, and magnesium concentrations on the oxidation rate. The regression analysis yields a comprehensive equation:  $k = -0.01Al - 4.06Cu - 15.71Mg + 4.52Al \cdot Cu + 17.01Al \cdot Mg + 418.5Cu \cdot Mg - 447.7Al \cdot Cu \cdot Mg$ , with statistically significant results ( $p < 0.05$ ) for all terms. An increase in magnesium concentration was found to enhance the oxidation rate, implying a higher alloy susceptibility to oxidation. These findings underline the value of the EVD method and regression analysis in alloy property optimization, thus aiding in the design of aluminum alloys with improved oxidation resistance.

**Keywords:** 2024 aluminum alloy, Mg content, alloy optimization, extreme vertices design, oxidation behavior.

## 1. Introduction

Aluminum alloys are widely used in industry due to their desirable mechanical and physical properties. Among the aluminum alloys, the 2000 series alloys, particularly the 2024 alloy, have high strength and excellent fatigue resistance, making them attractive for aerospace and automotive applications. However, the optimization of these properties requires the development of new alloy designs<sup>1-4</sup>. The aluminum alloy AA 2024 is valued for its mechanical strength characteristics, with the primary hardening mechanism attributed to the precipitation of  $Al_2Cu$  and  $Al_2CuMg$ . Given this intrinsic relationship, the concentrations of copper (Cu) and magnesium (Mg) in the alloy play a pivotal role in determining the quantity and nature of the precipitates formed. Therefore, a strategic approach to adjusting and optimizing the properties of the AA 2024 alloy involves manipulating these Cu and Mg proportions.

One method to optimize the properties of aluminum alloys is the Extreme Vertices Design (EVD) coupled with linear regression. This method allows for the development of new alloys with desirable properties by exploring the composition space and predicting the behavior of the alloy based on a mathematical model. In the field of materials science and engineering, the EVD methodology has emerged as a pivotal tool for optimizing and investigating various materials and processes. Its applications range from optimizing the mechanical properties of Glass Reinforced Concrete (GRC) mixtures<sup>5</sup> to the precise determination of optimal Al-Si-Ni powder ratios for achieving uniform weld

microstructures without delamination<sup>6</sup>. In the area of alloy design, it was identified that the only publication employing the EVD is a study focused on powder metallurgy to produce the W-Ni-Cu alloy. The study found that the multiple correlation coefficient  $R^2$  of the regression equation is about one and that the EVD method can be used to optimize the composition of W-Ni-Cu alloys and predict the properties of the alloys. These results suggest that the use of EVD in alloy design should be more widely disseminated, as it is an effective technique that has shown promising results<sup>7</sup>. Surprisingly, despite the notable efficiency of the EVD technique, it remains extremely underpublicized. Research in metallurgy, without the application of this method, often relies on trial and error approaches, indicating that metallic alloys are in need of optimization.

The 2024 alloy solution heat treatment is typically carried out at around 500°C for 4-16 hours<sup>8</sup>. However, in some cases, prolonged exposure to elevated temperatures during the process can result in undesirable oxidation of the alloy. One major challenge in the development of aluminum alloys is the occurrence of oxidation during the solution heat treatment<sup>9</sup>. In previous experiments in our laboratory, it was shown that the addition of magnesium to the alloy had been identified as a major cause of oxidation during the treatment, which can lead to undesirable changes in the properties of the alloy. In this study, we manufactured alloys with different chemical compositions. As a result, we observed the formation of a dark oxide layer on the surface of the alloy, which became thicker with increasing magnesium content after the solubilization treatment at 520°C for 12 hours.

\*e-mail: antunes@ita.br

We investigated the parabolic rate law to address this challenge, establishing a parabolic relationship between the specific oxidation rate and time.

Understanding the oxidation behavior of alloys during the solubilization treatment is critical to avoid excessive oxidation and limit the composition range for subsequent optimization of their mechanical properties. To achieve this goal, the parabolic rate equation, given by  $m/A = k \cdot t^{(1/2)}$ , can be used to describe the kinetics of oxidation behavior, where  $m/A$  represents the specific mass increment ( $\text{g}\cdot\text{cm}^{-2}$ ),  $t$  is time (h), and  $k$  ( $\text{g}\cdot\text{cm}^{-2}\cdot\text{h}^{(1/2)}$ ) is the specific oxidation rate constant of the material.

Therefore, this work aimed to determine the composition range and treatment time without significant oxidation during solubilization for subsequent optimization of the mechanical properties of the alloy by using the parabolic rate equation to study the oxidation behavior of the alloy.

## 2. Materials and Methods

In the present study, the R package “mixexp” was used to design the composition of the alloys. Specifically, the “Xvert” function was employed to create the experimental design using the Extreme Vertices Design approach<sup>10</sup>. The design was created using three factors, with lower and upper limits defined as 0.93 wt.% for Al, 0.04 wt.% for Cu, 0.01 wt.% for Mg, and 0.95 wt.% for Al, 0.06 wt.% for Cu, and 0.03 wt.% for Mg, respectively. Overall, this approach allowed for systematically exploring the design space and identifying promising compositions for subsequent processing and testing. Figure 1 shows the distribution of experimental points in the ternary diagram, and Table 1 presents the experimental design table obtained by the Xvert function. The central point was triplicated to improve the fitting of the experimental model.

Nine ingots were produced using primary aluminum, aluminum-copper master alloys with 32wt.% copper and aluminum-magnesium master alloy with 90wt.% magnesium. The proportions for each alloy composition were calculated, and the melting charge was prepared. For each ingot, primary aluminum was initially melted at 720°C, followed by adding the aluminum-copper master alloy. After 15 minutes of dissolution, the bath was stirred, degassed with hexachloroethane, and removed the slag. Then, a flux of magnesium chloride and potassium chloride was added to prevent magnesium oxidation, followed by the addition of aluminum-magnesium master alloy. After 5 minutes of dissolution, the bath was stirred, the slag was removed, and

the liquid metal was cast into a refractory-coated conical steel ingot mold. The weight of each ingot was approximately 90 grams. The nominal chemical composition of the produced ingots is presented below.

The ingots were sliced using a metallographic cutting disc and squared to obtain approximately 20 x 20 mm samples. Subsequently, the samples were subjected to an oxidation treatment at a temperature of 520°C for varying durations of 1, 2, 3, 4, 5, 7, 9, and 28 hours. The initial mass of each sample and the mass after each treatment were measured using an analytical balance. A dataset was created with the mass increment for each composition at each treatment time, totaling 72 instances.

In this study, the parabolic rate equation was used to calculate the value of  $k$  for each ingot. The equation is expressed as  $m/A = k \cdot t^{(1/2)}$ , where  $m/A$  represents the specific mass increment ( $\text{g}\cdot\text{cm}^{-2}$ ),  $t$  is time (h), and  $k$  ( $\text{g}\cdot\text{cm}^{-2}\cdot\text{h}^{(1/2)}$ ) is a constant related to the material properties and oxidation conditions. This approach allowed for the evaluation of the oxidation behavior of the alloys and the identification of the composition with the best oxidation resistance.

In this study, the modeling approach used the MixModel function from the R package “mixexp”. The response variable “ $k$ ”, representing the specific oxidation rate constant, was modeled as a function of Al, Cu, and Mg alloy components.

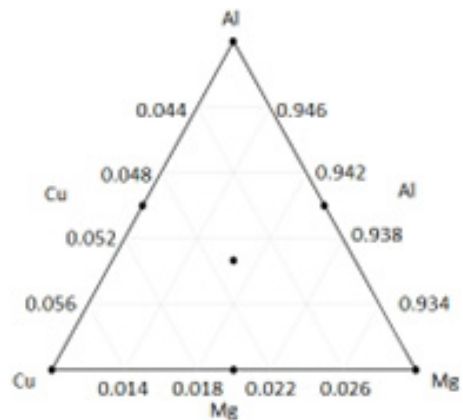


**Figure 1.** Ternary plot of the experimental design created using the “Xvert” function from the R package “mixexp” with the Extreme Vertices Design approach. The central point represents three superimposed points.

**Table 1.** Chemical composition of produced ingots in weight percent of Al, Cu, and Mg.

Alloy	Al / wt.%	Cu / wt.%	Mg / wt.%
A1	93.0	6.0	1.0
A2	94.0	5.0	1.0
A3	95.0	4.0	1.0
A4	93.7	4.7	1.7
A5	93.7	4.7	1.7
A6	93.7	4.7	1.7
A7	93.0	5.0	2.0
A8	94.0	4.0	2.0
A9	93.0	4.0	3.0

The MixModel function allowed for fitting a regression model to estimate the relationship between the alloy components and the specific oxidation rate constant.

### 3. Results and Discussion

Figure 2 displays the specific mass increment as a function of oxidation time for nine different alloys (A1 to A9). Each data point represents experimental measurements, while the lines represent regression curves fitted to the data for each alloy. The y-axis represents the specific mass increment ( $\text{g}/\text{cm}^2$ ), and the x-axis represents the oxidation time (h). The legend in the top-right corner of the graph provides a color/shape correspondence for each alloy.

The graph clearly shows variations in the specific mass increment among the different alloys throughout the oxidation process. Notably, alloys A7 and A9 exhibit a significant increase in the specific mass increment compared to the other alloys, indicating a higher susceptibility to oxidation. On the other hand, alloys A1, A2, and A3 demonstrate a relatively low specific mass increment, suggesting a higher oxidation resistance. It is worth noting that the inclination of the regression lines represents the oxidation rate constant ( $k$ ), with steeper slopes indicating higher values of  $k$ . Therefore, a greater slope of the regression line implies a higher  $k$  and, consequently, lower resistance to oxidation for the respective alloy.

The regression analysis results, presented in Table 2, provide each alloy's oxidation rate constant ( $k$ ) values and the adjusted R-squared and p-value of the regression fit. Based on the table results, we can conclude that the regression model fit is statistically reliable for most alloys. It is indicated by the adjusted coefficient of determination (Adjusted R-squared) values being close to 1, suggesting that the model explains a substantial portion of the data variability.

Additionally, the p-values of the model fit are consistently low for all alloys, signifying the statistical significance of the fit. Lower p-values reflect higher statistical confidence in the model fit. In this case, the p-values range from  $2.5\text{E-}07$  to  $2.8\text{E-}05$ , all providing statistically solid evidence that the model effectively describes the relationship between the oxidation rate ( $k$ ) and the oxidation time of the alloys.

To further understand the oxidation behavior of the alloys, we obtained the coefficient estimates ( $k$ ) through regression analysis, as presented in the previous discussion. Building upon these results, we now investigate the influence of chemical concentration on the value of  $k$ . By examining the coefficient estimates and their corresponding significance, we can gain valuable insights into how chemical composition changes impact the oxidation rate. Table 3 presents the coefficient estimates, standard errors, t-values, and p-values for each chemical concentration variable in the regression analysis model. The model will be a polynomial involving the concentrations of Al, Cu, and Mg in the sample and the interaction terms Al:Cu, Al:Mg, Cu:Mg, and Al:Cu:Mg.

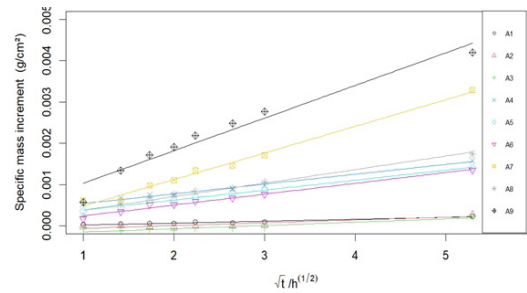


**Figure 2.** Specific mass increment as a function of oxidation time for different alloys.

**Table 2.** Regression Analysis Results for Specific Mass Increment of the Alloys.

Alloy	$k / \text{g} \cdot \text{cm}^{-2} \cdot \text{h}^{-1/2}$	Adjusted R-squared	p-value
A1	0.47E-04	0.93	5.8E-05
A2	0.67E-04	0.77	2.5E-03
A3	0.79E-04	0.85	7.3E-04
A4	2.37E-04	0.99	2.5E-07
A5	2.63E-04	0.98	8.0E-07
A6	2.63E-04	0.98	8.0E-07
A7	6.46E-04	0.99	3.2E-04
A8	3.29E-04	0.97	5.2E-06
A9	7.91E-04	0.95	2.8E-05

**Table 3.** Coefficient Estimates of the Regression Analysis for the Influence of Chemical Concentration on  $k$ .

Coefficients	Estimate	Std. Error	t value	Pr(> t )
Al	-1.157e-02	1.728e-03	-6.698	0.0216
Cu	-4.062e+00	5.405e-01	-7.515	0.0172
Mg	-1.571e+01	1.927e+00	-8.153	0.0147
Al:Cu	4.519e+00	6.053e-01	7.466	0.0175
Al:Mg	1.701e+01	2.092e+00	8.132	0.0148
Cu:Mg	4.185e+02	4.668e+01	8.965	0.0122
Al:Cu:Mg	-4.477e+02	5.010e+01	-8.937	0.0123

The coefficient estimates provide insights into the magnitude and direction of the effect of each chemical concentration on the oxidation rate constant ( $k$ ). The  $t$ -values and  $p$ -values indicate the statistical significance of these effects, providing evidence for the influence of chemical concentrations on the oxidation process.

Firstly, the standard errors represent the precision of the coefficient estimates. Smaller values indicate a higher level of precision, suggesting a more reliable estimation of the true population coefficient. Our analysis shows relatively tiny standard errors for most coefficients, indicating good precision in estimating their values. Secondly, the  $t$ -values are calculated by dividing the coefficient estimate by its standard error. A higher absolute  $t$ -value indicates a greater coefficient significance in the model. In our results, several coefficients exhibit large  $t$ -values, suggesting their strong influence on the oxidation rate. Lastly, the  $p$ -values reflect the statistical significance of each coefficient. They indicate the probability of observing a coefficient as extreme as the one estimated, assuming the null hypothesis of no relationship between the predictor variable and the response variable. In our study, most coefficients have  $p$ -values below the conventional significance level of 0.05, providing strong evidence against the null hypothesis and supporting a relationship between the chemical concentrations and the oxidation rate.

The results, taken together, indicate that the regression model effectively describes the data and provides meaningful insights into the influence of chemical concentrations on the oxidation rate of the alloys. The statistically significant coefficients and their precise estimation support the model's reliability, reinforcing the understanding of the complex interplay between alloy composition and oxidation behavior.

The regression analysis model has resulted in a comprehensive equation that explains the specific oxidation rate constant ( $k$ ) in terms of the chemical compositions of the alloys. The equation provides detailed insights into the combined and individual effects of Al, Cu, and Mg on the oxidation rate. This complex relationship between the alloy composition and its oxidation behavior underscores the importance of a delicate balance in alloy composition to optimize its resistance to oxidation. It's important to note that this equation is constrained to the parameters of the experimental design, with the composition limits defined explicitly as 0.93 to 0.95 wt.% for Al, 0.04 to 0.06 wt.% for Cu, and 0.01 to 0.03 wt.% for Mg, and it is strictly applicable within this boundary.

$$k = -0.01Al - 4.06Cu - 15.71Mg + 4.52Al.Cu + 17.01Al.Mg + 418.5Cu.Mg - 447.7Al.Cu.Mg$$

Figure 3 displays the mixture effect plots illustrating the impact of aluminum ( $x_1$ ), Copper ( $x_2$ ), and Magnesium ( $x_3$ ) concentrations on the oxidation rate constant ( $k$ ). Each plot represents these chemical components' individual and combined effects on  $k$ . This graphical representation facilitates the identification of trends and interactions among the component concentrations, contributing to a better understanding of how each component and its combinations influence the material's resistance to oxidation. It can be observed that from the center, an increase in the amount of magnesium causes a significant increase in the value of  $k$ . At the same time, the increment of the other elements is less significant.

Figure 4 shows a Pseudo Component Ternary Plot of the Regression Model. The plot shows the relationship between the alloy components Al (aluminum), Cu (copper), and Mg (magnesium) and the specific oxidation rate constant ( $k$ ). The plot is based on the fitted regression model and represents the predicted values of  $k$  for different combinations of alloy compositions. The axis represents Al, Cu, and Mg concentrations, while the color intensity represents the specific oxidation rate constant ( $k$ ). The contour lines indicate the regions of similar  $k$  values. The plot is generated using the ModelPlot function from the R package "mixexp".

Notice that as the amount of magnesium increases, the  $k$  index also increases, indicating lower resistance to oxidation of the alloy. Additionally, it is essential to observe that the contour lines in the magnesium corner are not parallel to the copper axis, suggesting an interaction between magnesium and copper. This interaction implies that an increase in magnesium and copper concentrations contributes to an increase in  $k$ , although the effect is more pronounced for magnesium.

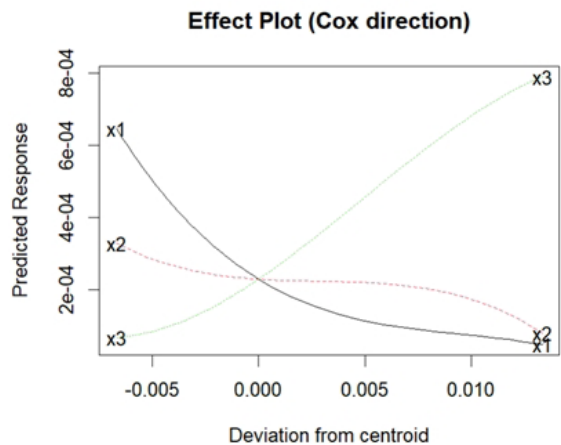


Figure 3. Mixture Effect Plots for Aluminum ( $x_1$ ), copper ( $x_2$ ), and magnesium ( $x_3$ ) concentrations.

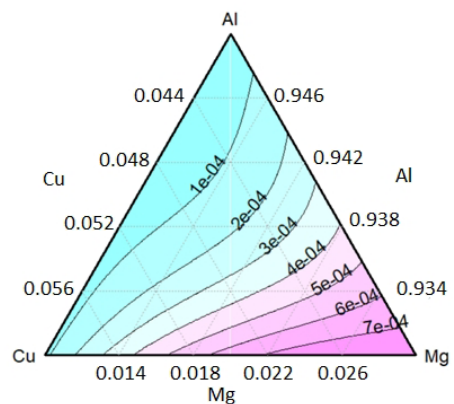


Figure 4. Pseudo Component Space Ternary plot of the Regression Model. The plot shows the relationship between the alloy components Al (aluminum), Cu (copper), and Mg (magnesium) and the specific oxidation rate constant ( $k$ ).

Further discussion on this observation can be found in Figure 3. We can correlate Figures 3 and 4 as follows: If we increase variables  $x_1$ ,  $x_2$ , and  $x_3$ , i.e., deviate from the centroid in the positive direction, the value of  $k$  increases significantly for  $x_3$ , while it decreases for  $x_1$  and  $x_2$ . However, if we decrease variables  $x_1$ ,  $x_2$ , and  $x_3$ , i.e., deviate from the centroid in the negative direction, the value of  $k$  increases considerably for variable  $x_1$ , increases very little for variable  $x_2$ , and decreases for variable  $x_3$ .

Within the confines of this work, we did not specifically identify the oxides formed on the alloy surface. Based on observations and existing literature, we speculate that the oxidation rate might be influenced by the phases present on the surface. The phases of the aluminum matrix, along with frequently observed precipitates in the alloy such as  $Al_2Cu$  and  $Al_2CuMg$ , could play a significant role in this context. The proportion of these phases and their potential mode of oxidation (be it through pure oxides, represented by  $X_mO_n$ , or mixed compounds indicated by  $X_mY_nO_p$ ) might relate to the value of the rate constant  $k$ . Moreover, it's relevant to consider a potential kinetic influence of these phases, as they might have originated during the alloy's slow solidification. At the oxidation temperature used, such phases might gradually dissolve into the alloy, theoretically influencing the oxidation kinetics. However, the exact significance of each of the mentioned phenomena remains unknown to us. We emphasize that our analysis is a macroscopic attempt to elucidate potential microscopic effects suggested above.

## 4. Conclusions

This study investigated the optimization of aluminum alloy properties, specifically focusing on the 2024 alloy, widely used in aerospace and automotive applications. The Extreme Vertices Design (EVD) coupled with linear regression proved to be an effective method for designing new alloys and predicting their properties. By systematically exploring the composition space using EVD, we identified promising compositions for subsequent processing and testing.

One major challenge in aluminum alloy development is the occurrence of oxidation during the solubilization heat treatment process. Our findings revealed that increased magnesium content resulted in a higher susceptibility to oxidation, forming a thick oxide layer on the alloy's surface. We studied the oxidation behavior using the parabolic rate equation and established a relationship between the specific oxidation rate and time.

The findings emphasized the importance of carefully considering the magnesium content to avoid undesirable oxidation during the solubilization heat treatment. However, future studies should focus on evaluating the beneficial effects of beryllium on oxidation resistance during the solubilization process of aluminum alloys, as mentioned by Zhu et al.<sup>11</sup>.

## 5. References

1. Razooghi AI, Abbas NM, Ghazi SS. Influence of multi extrusion die process on mechanical and chemical behavior of 2024-T3 alloy. *Int. J Appl Mech Eng.* 2022;27(3):163-70. <http://dx.doi.org/10.2478/ijame-2022-0042>.
2. Özkavak V, İnce M, Bıçaklı EE. Prediction of mechanical properties of the 2024 aluminum alloy by using machine learning methods. *Arab J Sci Eng.* 2023;48(3):2841-50. <http://dx.doi.org/10.1007/s13369-022-07009-8>.
3. Srivastava AK, Maurya NK, Maurya M, Dwivedi SP, Saxena A. Effect of multiple passes on microstructural and mechanical properties of surface composite Al 2024/SiC produced by friction stir processing. *Ann Chim.* 2020;44(6):421-6. <http://dx.doi.org/10.18280/acsm.440608>.
4. Cabral Miramontes JA, Martínez Aparicio BS, Olguín Coca FJ, López León LD, Estupiñán-López FH, Gaona Tiburcio C, et al. Corrosion resistance of Alloy 2024 anodized on sulfuric-citric acid. *ECS Trans.* 2019;94(1):73-80. <http://dx.doi.org/10.1149/09401.0073ecst>.
5. Mishra S, Sharma L, Chhibber R. Modelling and thermophysical properties of  $TiO_2$ - $SiO_2$ -CaO and  $SiO_2$ -CaO-MgO based electrode coatings for offshore applications. *Silicon.* 2023;15(16):7015-37. <http://dx.doi.org/10.1007/s12633-023-02559-4>.
6. Wang Y-Y, Yang X-N, Shi S-Y, Wu Z, Han R-H, Qi H-B. Laser welding 6061 aluminum alloy with laser cladding powder. *J Laser Appl.* 2021;33(2):022006. <http://dx.doi.org/10.2351/7.0000217>.
7. Xin S, Guo C, Dong H, Jing R. Application of mixture experiments in the composition design of W-Ni-Cu alloys. *Mater Sci Eng Powder Metall.* 2016;21(4):527-33.
8. Pannaray S, Wisutmethangoon S, Plookphol T, Wannasin J. Microstructure evolution during solution heat treatment of semisolid cast 2024 aluminum alloy. *Adv Mat Res.* 2011;339(1):714-7. <http://dx.doi.org/10.4028/www.scientific.net/AMR.339.714>.
9. Solem CKW, Vullum P, Ebadi M, Tranell G, Aune R. The role of  $CO_2$  in the oxidation-protection of Mg-containing aluminum alloys. *Metall Mater Trans, B, Process Metall Mater Proc Sci.* 2022;53(4):1967. <http://dx.doi.org/10.1007/s11663-022-02524-3>.
10. Lawson J, Willden C. Mixture experiments in R using mixexp. *J Stat Softw.* 2016;72(2). <http://dx.doi.org/10.18637/jss.v072.c02>.
11. Zhu X, Blake P, Dou K, Ji S. Strengthening die-cast Al-Mg and Al-Mg-Mn alloys with Fe as a beneficial element. *Mater Sci Eng A.* 2018;732:240-50. <http://dx.doi.org/10.1016/j.msea.2018.07.005>.